

## Exclusive diffractive production of $\pi^+\pi^-$ continuum and resonances within tensor pomeron approach

Piotr Lebiedowicz<sup>1,\*</sup>, Otto Nachtmann<sup>2</sup>, and Antoni Szczurek<sup>1,\*\*</sup>

<sup>1</sup>*Institute of Nuclear Physics Polish Academy of Sciences, PL-31342 Kraków, Poland*

<sup>2</sup>*Institut für Theoretische Physik, Universität Heidelberg, D-69120 Heidelberg, Germany*

**Abstract.** We discuss exclusive central diffractive dipion production in proton-(anti)proton collisions at high energies. The calculation is based on a tensor pomeron model and the amplitudes for the processes are formulated in an effective field-theoretic approach. We include the purely diffractive dipion continuum, and the scalar and tensor resonances decaying into the  $\pi^+\pi^-$  pairs as well as the photoproduction contributions ( $\rho^0$ , Drell-Söding). We discuss how two pomerons couple to tensor meson  $f_2(1270)$  and the interference effects of resonance and dipion continuum. The theoretical results are compared with CDF and CMS experimental data. We show the influence of the experimental cuts on the integrated cross section and on various differential distributions for outgoing particles. We find that the relative contribution of resonant  $f_2(1270)$  and dipion continuum strongly depends on the cut on proton transverse momenta (or four-momentum transfer squared  $t_{1,2}$ ) which may explain some controversial observations made by different ISR experiments in the past. The cuts may play then the role of a  $\pi\pi$  resonance filter. We suggest some experimental analyses to fix model parameters related to the pomeron-pomeron-meson coupling.

### 1 Introduction

Central production mediated by the “fusion” of two exchanged pomerons [1, 2] is an important diffractive process for the investigation of properties of di-pion resonances, in particular, for search of gluonic bound states (glueballs). The experimental groups such as the COMPASS [3, 4], ISR [5, 6], STAR [7, 8], CDF Tevatron [9], ALICE [10], and CMS [11] all show visible structures in the  $\pi^+\pi^-$  invariant mass. Some time ago two of us have formulated a Regge-type model of the dipion continuum for the exclusive reaction  $pp \rightarrow pp\pi^+\pi^-$  with parameters fixed from phenomenological analysis of total and elastic  $NN$  and  $\pi N$  scattering [13]. The number of free model parameters is then limited to a parameter of form factor describing off-shellness of the exchanged pion. The model was extended to include rescattering corrections due to  $pp$  nonperturbative interaction [12, 14]. The exclusive reaction  $pp \rightarrow pp\pi^+\pi^-$  constitutes an irreducible background to the scalar  $\chi_{c0}$  meson production [14]. These model studies were extended also to exclusive  $K^+K^-$  production [15]. The largest uncertainties in the model are due to the unknown off-shell pion form factor and the absorption effects; see Ref. [16].

\*e-mail: Piotr.Lebiedowicz@ifj.edu.pl

\*\*Also at University of Rzeszów, PL-35959 Rzeszów, Poland.

Such an approach gives correct order of magnitude cross sections, however, does not include resonance contributions which interfere with the continuum contribution.

First calculations of central exclusive diffractive production of  $\pi^+\pi^-$  continuum together with the dominant scalar  $f_0(500)$ ,  $f_0(980)$ , and tensor  $f_2(1270)$  resonances was performed in Ref. [1]. Here we use the tensor-pomeron model formulated in [17]; see also [18]. In this model pomeron exchange is effectively treated as the exchange of a rank-2 symmetric tensor. In [19] we show that the tensor pomeron is consistent with the STAR  $pp$  elastic scattering data [20]. In Ref. [21] the model was applied to the diffractive production of several scalar and pseudoscalar mesons in the reaction  $pp \rightarrow ppM$ . The corresponding pomeron-pomeron-meson coupling constants are not known and have been fitted to existing WA102 experimental data. In most cases one has to add coherently amplitudes for two pomeron-pomeron-meson couplings with different orbital angular momentum and spin of two ‘‘pomeron particles’’. <sup>1</sup> In [22] an extensive study of the photoproduction reaction  $\gamma p \rightarrow \pi^+\pi^- p$  was presented. The resonant ( $\rho^0 \rightarrow \pi^+\pi^-$ ) and non-resonant (Drell-Söding) photon-pomeron/reggeon  $\pi^+\pi^-$  production in  $pp$  collisions was studied in [23].

The identification of glueballs can be very difficult; see e.g. [24]. The partial wave analyses of future experimental data could be used in this context. Also the studies of different decay channels in central exclusive production would be very valuable. One of the possibilities is the  $pp \rightarrow pp\pi^+\pi^-\pi^+\pi^-$  reaction being analysed at the LHC. In Ref. [25] we analysed the exclusive diffractive production of four-pion via the intermediate  $\sigma\sigma$  and  $\rho\rho$  states (for a related work see [26]).

## 2 Sketch of formalism

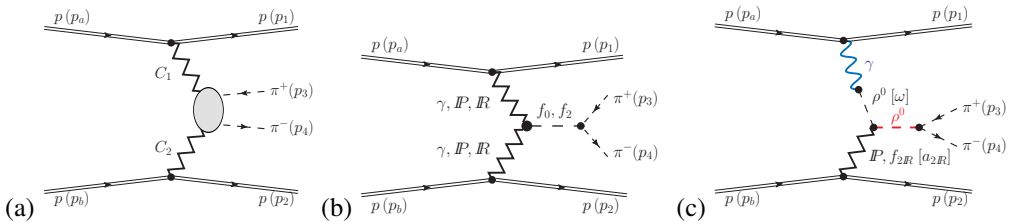


**Figure 1.** Diagram (a): Generic Born level diagram for central exclusive continuum  $\pi^+\pi^-$  production in proton-(anti)proton collisions. Here we labelled the exchange objects by their charge conjugation numbers  $C_1, C_2 \in \{+1, -1\}$ . Diagram (b): The double-pomeron/reggeon and photon mediated central exclusive scalar and tensor resonance production and their subsequent decays into  $\pi^+\pi^-$ . Diagram (c): The  $\rho^0$  photoproduction mechanism.

The Born level diagrams for the continuum and resonant  $\pi^+\pi^-$  production are shown in Fig. 1. The purely diffractive amplitude is a sum of continuum amplitude and the amplitudes with the  $s$ -channel resonances with very restrictive quantum numbers  $I^G J^{PC} = 0^+(\text{even})^{++}$ :

$$\mathcal{M}_{pp \rightarrow pp\pi^+\pi^-} = \mathcal{M}_{pp \rightarrow pp\pi^+\pi^-}^{\pi\pi\text{-continuum}} + \mathcal{M}_{\lambda_a\lambda_b \rightarrow \lambda_1\lambda_2\pi^+\pi^-}^{(\mathbb{P}\mathbb{P} \rightarrow f_0 \rightarrow \pi^+\pi^-)} + \mathcal{M}_{\lambda_a\lambda_b \rightarrow \lambda_1\lambda_2\pi^+\pi^-}^{(\mathbb{P}\mathbb{P} \rightarrow f_2 \rightarrow \pi^+\pi^-)}. \quad (1)$$

<sup>1</sup>We wish to emphasize that the tensorial pomeron can, at least, equally well describe the WA102 experimental data on the exclusive meson production as the less theoretically justified vectorial pomeron frequently used in the literature. The existing low-energy experimental data do not allow to clearly distinguish between the two models as the presence of subleading reggeon exchanges is at low energies very probable for many  $pp \rightarrow ppM$  reactions.

For instance, the Born (no absorption effects) amplitude for the process  $pp \rightarrow pp(\mathbb{P}\mathbb{P} \rightarrow f_2 \rightarrow \pi^+\pi^-)$  can be written in the effective field-theoretic approach as

$$\begin{aligned} \mathcal{M}_{\lambda_a \lambda_b \rightarrow \lambda_1 \lambda_2 \pi^+ \pi^-}^{(\mathbb{P}\mathbb{P} \rightarrow f_2 \rightarrow \pi^+ \pi^-)} &= (-i) \bar{u}(p_1, \lambda_1) i \Gamma_{\mu_1 \nu_1}^{(\mathbb{P}pp)}(p_1, p_a) u(p_a, \lambda_a) i \Delta^{(\mathbb{P})\mu_1 \nu_1, \alpha_1 \beta_1}(s_1, t_1) \\ &\quad \times i \Gamma_{\alpha_1 \beta_1, \alpha_2 \beta_2, \rho \sigma}^{(\mathbb{P}\mathbb{P}f_2)}(q_1, q_2) i \Delta^{(f_2)\rho \sigma, \alpha \beta}(p_{34}) i \Gamma_{\alpha \beta}^{(f_2 \pi \pi)}(p_3, p_4) \\ &\quad \times i \Delta^{(\mathbb{P})\alpha_2 \beta_2, \mu_2 \nu_2}(s_2, t_2) \bar{u}(p_2, \lambda_2) i \Gamma_{\mu_2 \nu_2}^{(\mathbb{P}pp)}(p_2, p_b) u(p_b, \lambda_b), \end{aligned} \quad (2)$$

where  $t_1 = (p_1 - p_a)^2$ ,  $t_2 = (p_2 - p_b)^2$ ,  $s_1 = (p_a + q_2)^2 = (p_1 + p_{34})^2$ ,  $s_2 = (p_b + q_1)^2 = (p_2 + p_{34})^2$ ,  $p_{34} = p_3 + p_4$ .  $\Delta^{(\mathbb{P})}$  and  $\Gamma^{(\mathbb{P}pp)}$  denote the effective propagator and proton vertex function, respectively, for the tensorial pomeron. For the explicit expressions, see Sec. 3 of [17]. The pomeron-pomeron- $f_2$  vertex is the most complicated element of our amplitude (2). In Ref. [1] we have considered all possible tensorial structures for the  $\mathbb{P}\mathbb{P}f_2$  coupling (see Appendix A of [1])

$$i \Gamma_{\mu\nu, \kappa\lambda, \rho\sigma}^{(\mathbb{P}\mathbb{P}f_2)}(q_1, q_2) = \left( i \Gamma_{\mu\nu, \kappa\lambda, \rho\sigma}^{(\mathbb{P}\mathbb{P}f_2)(1)} |_{bare} + \sum_{j=2}^7 i \Gamma_{\mu\nu, \kappa\lambda, \rho\sigma}^{(\mathbb{P}\mathbb{P}f_2)(j)}(q_1, q_2) |_{bare} \right) \tilde{F}^{(\mathbb{P}\mathbb{P}f_2)}(q_1^2, q_2^2, p_{34}^2). \quad (3)$$

Other details as form of form factors, the tensor-meson propagator  $\Delta^{(f_2)}$  and the  $f_2\pi\pi$  vertex are given in Refs. [1, 17]. The production of the  $f_2$  meson via  $\mathbb{P}f_{2\mathbb{R}}$ ,  $f_{2\mathbb{R}}\mathbb{P}$ , and  $f_{2\mathbb{R}}f_{2\mathbb{R}}$  fusion can be treated in an analogous way to the  $\mathbb{P}\mathbb{P}$  fusion.

We consider also the production of  $\rho(770)$  resonance produced by photon-pomeron/reggeon mechanism studied in detail in [23], see the panel (c) in Fig. 1. In the amplitude for the  $\gamma p \rightarrow \rho^0 p$  subprocess we included both pomeron and  $f_{2\mathbb{R}}$  exchanges. The  $\mathbb{P}\rho\rho$  vertex is given in [17] by formula (3.47). The coupling parameters of tensor pomeron/reggeon exchanges was fixed based on the HERA experimental data for the  $\gamma p \rightarrow \rho^0 p$  reaction. In [23] we showed that the resonant contribution interfere with the non-resonant (Drell-Söding)  $\pi^+\pi^-$  continuum and produces a skewing of the  $\rho(770)$ -meson line shape. Due to the photon propagators occurring in diagrams we expect these processes to be most important when at least one of the protons undergoes only a very small  $|t_{1,2}|$ .

### 3 Selected results

We start from a discussion of some dependences for the central exclusive production of the  $f_2(1270)$  meson. For detailed study of  $f_2(1270)$  production see Ref. [1]. In Fig. 2 we present results for individual pomeron-pomeron- $f_2$  coupling terms (there are 7 possible terms [1]) at  $\sqrt{s} = 200$  GeV and  $|\eta_\pi| < 1$ . The different predictions differ considerably which could be checked experimentally. We show that only in two cases ( $j = 2$  and 5) the cross section  $d\sigma/d|t_{1,2}|$  vanishes when  $|t_{1,2}| \rightarrow 0$ . In [1] we tried to understand whether one can approximately describe the dipion invariant mass distribution observed by different experiments assuming only one of the seven possible  $\mathbb{P}\mathbb{P}f_2$  tensorial couplings. We found that the feature of the  $\pi^+\pi^-$  distribution depends on the cuts used in a particular experiment (usually the  $t$  cuts are different for different experiments). As can be clearly seen from Fig. 3 different  $\mathbb{P}\mathbb{P}f_2$  couplings generate different interference patterns around  $M_{\pi\pi} \sim 1.27$  GeV. A sharp drop around  $M_{\pi\pi} \sim 1$  GeV is attributed to the interference of  $f_0(980)$  and continuum. We can observe that the  $j = 2$  coupling gives results close to those observed by the CDF Collaboration [9]. In this preliminary study we did not try to fit the existing data [9] by mixing different couplings because the CDF data are not fully exclusive (the outgoing  $p$  and  $\bar{p}$  were not measured). The calculations were done at Born level and the absorption corrections were taken into account by multiplying the cross section by a common factor  $\langle S^2 \rangle$  obtained from [16]. The two-pion continuum was fixed by choosing a form factor for the off-shell pion  $\hat{F}_\pi(k^2) = \frac{\Lambda_{off,M}^2 - m_\pi^2}{\Lambda_{off,M}^2 - k^2}$  and  $\Lambda_{off,M} = 0.7$  GeV.

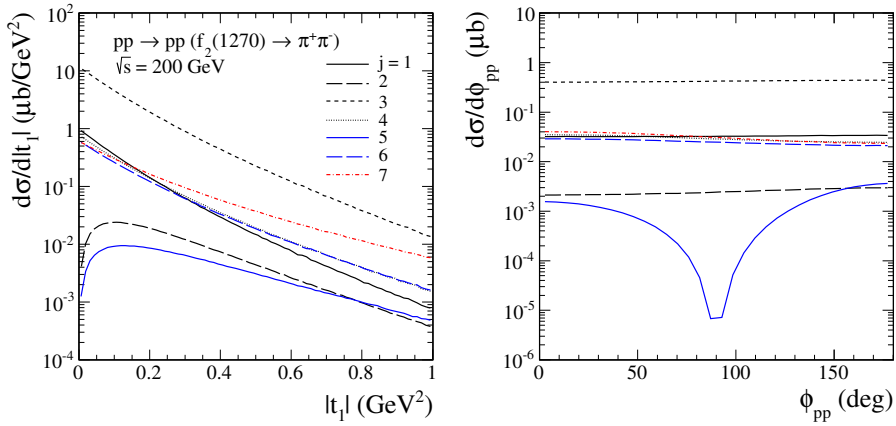


**Figure 2.** The distribution in transferred four-momentum squared between the initial and final protons (left panel) and the distribution in azimuthal angle between the outgoing protons (right panel) at  $\sqrt{s} = 200$  GeV and  $|\eta_\pi| < 1$ . We show the individual contributions of the different pomeron-pomeron- $f_2(1270)$  couplings:  $j = 1$  (the black solid line),  $j = 2$  (the black long-dashed line),  $j = 3$  (the black dashed line),  $j = 4$  (the black dotted line),  $j = 5$  (the blue solid line),  $j = 6$  (the blue long-dashed line), and  $j = 7$  (the red dot-dashed line). For illustration the results have been obtained with coupling constants  $g_{\mathbb{P}\mathbb{P}f_2}^{(j)} = 1.0$ . No absorption effects were included here.

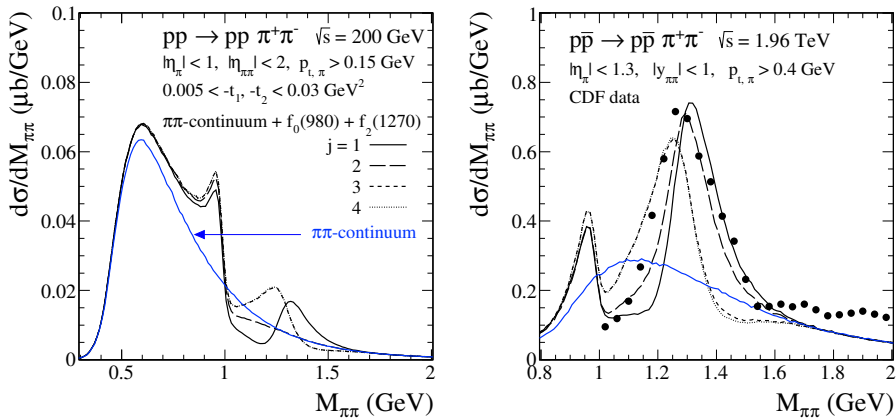


**Figure 3.** Two-pion invariant mass distribution for the STAR [7] (left) and CDF [9] (right) kinematics. The individual contributions of different  $\mathbb{P}\mathbb{P}f_2$  couplings ( $j = 1, \dots, 4$ ) are compared with the CDF data [9]. The Born calculations for  $\sqrt{s} = 200$  GeV and  $\sqrt{s} = 1.96$  TeV were multiplied by the gap survival factors  $\langle S^2 \rangle = 0.2$  and  $\langle S^2 \rangle = 0.1$ , respectively. The blue solid lines represent the non-resonant continuum contribution only ( $\Lambda_{off,M} = 0.7$  GeV) while the black lines represent a coherent sum of non-resonant continuum,  $f_0(980)$  and  $f_2(1270)$  resonant terms.

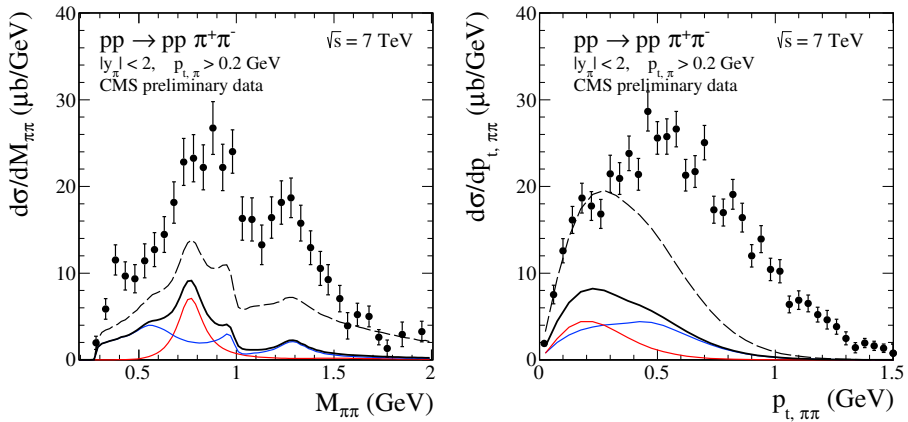


**Figure 4.** The distributions for two-pion invariant mass (left panel) and transverse momentum of the pion pair (right panel) for the CMS kinematics at  $\sqrt{s} = 7$  TeV. Both photoproduction (red line) and purely diffractive (blue line) contributions multiplied by the factors  $\langle S^2 \rangle = 0.9$  and  $\langle S^2 \rangle = 0.1$ , respectively, are included. The complete results correspond to the black solid line ( $\Lambda_{off,M} = 0.7$  GeV) and the dashed line ( $\Lambda_{off,M} = 1.2$  GeV). The CMS preliminary data scanned from [11] are shown for comparison.

In Fig. 4 we show results including in addition to the non-resonant  $\pi^+\pi^-$  continuum, the  $f_2(1270)$  and the  $f_0(980)$  resonances, the contribution from photoproduction ( $\rho^0 \rightarrow \pi^+\pi^-$ , Drell-Söding mechanism), as well as the  $f_0(500)$  resonant contribution. Our predictions are compared with the CMS preliminary data [11]. Here the absorption effects lead to huge damping of the cross section for the purely diffractive term (the blue lines) and relatively small reduction of the cross section for the photoproduction term (the red lines). Therefore we expect one could observe the photoproduction contribution. The CMS measurement [11] is not fully exclusive and, inter alia, the  $M_{\pi\pi}$  and  $p_{t,\pi\pi}$  spectra contain contributions associated from other processes, e.g., when one or both protons undergoing dissociation. In addition we show results with  $\Lambda_{off,M} = 1.2$  GeV better adjusted to the new CMS data (see the dashed line). If we used this set for the STAR or CDF measurements our results there would be above the preliminary STAR data [7] at  $M_{\pi\pi} > 1$  GeV and in complete disagreement with the CDF data from [9]. Only purely central exclusive data expected from CMS-TOTEM and ATLAS-ALFA will allow to draw definite conclusions. The absorption effects due to  $pp$  and  $\pi p$  interactions, discussed in [16], lead to a significant modification of the shape of the distributions in  $\phi_{pp}$ ,  $p_{t,p}$ ,  $t_{1,2}$  and could also be tested by these experimental groups.

## 4 Conclusions

In our recent paper [1] we have analysed the exclusive central production of dipion continuum and resonances contributing to the  $\pi^+\pi^-$  pair production in proton-(anti)proton collisions in an effective field-theoretic approach with tensor pomerons and reggeons proposed in [17]. We have included the scalar  $f_0(500)$  and  $f_0(980)$  resonances, the tensor  $f_2(1270)$  resonance and the vector  $\rho(770)$  resonance in a consistent way. In the case of  $f_2(1270)$ -meson production via “fusion” of two tensor pomerons we have found [1] all (seven) possible  $\mathbb{P}\mathbb{P}f_2$  tensorial couplings. The different couplings give different results due to different interference effects of the  $f_2$  resonance and the dipion continuum contributions. We have shown that the resonance structures in the measured two-pion invariant mass spectra depend

on the cut on proton transverse momenta and/or on four-momentum transfer squared  $t_{1,2}$  used in an experiment. The model parameters of the optimal  $\mathbb{P}f_2$  coupling ( $j = 2$ ) have been roughly adjusted to the recent CDF and preliminary STAR experimental data and then used for the predictions for the ALICE, and CMS experiments. We have made estimates of cross sections for both the diffractive and photoproduction contributions. We have shown some differential distributions related to produced pions as well as some observables related to final state protons, e.g., different dependence on proton transverse momenta and azimuthal angle correlations between outgoing protons could be used to separate the photoproduction term, see [1]. Future experimental data on exclusive meson production at high energies should thus provide good information on the spin structure of the pomeron and on its couplings to the nucleon and the mesons.

This work was partially supported by the MNiSW Grant No. IP2014 025173 (Iuventus Plus) and the Polish National Science Centre grants DEC-2014/15/B/ST2/02528 and DEC-2015/17/D/ST2/03530.

## References

- [1] P. Lebiedowicz, O. Nachtmann, A. Szczurek, Phys. Rev. D **93**, 054015 (2016)
- [2] R. Fiore, L. Jenkovszky, R. Schicker, Eur. Phys. J. C **76**, 38 (2016)
- [3] A. Austregesilo (COMPASS Collaboration), AIP Conf. Proc. **1735**, 030012 (2016)
- [4] B. Grube, this Proceedings
- [5] T. Åkesson *et al.*, (AFS Collaboration), Nucl. Phys. B **264**, 154 (1986)
- [6] A. Breakstone *et al.* (ABCDHW Collaboration), Z. Phys. C **31**, 185 (1986); A. Breakstone *et al.* (ABCDHW Collaboration), Z. Phys. C **42**, 387 (1989); Erratum: Z. Phys. C **43**, 522 (1989); A. Breakstone *et al.* (ABCDHW Collaboration), Z. Phys. C **48**, 569 (1990)
- [7] L. Adamczyk, W. Guryń, J. Turnau, Int. J. Mod. Phys. A **29**, 1446010 (2014)
- [8] W. Guryń, this Proceedings
- [9] T. Aaltonen *et al.* (CDF Collaboration), Phys. Rev. D **91**, 091101 (2015)
- [10] R. Schicker (ALICE Collaboration), arXiv:1205.2588 [hep-ex].
- [11] CMS Collaboration, Report No. CMS-PAS-FSQ-12-004.
- [12] R. Staszewski, P. Lebiedowicz, M. Trzebiński, J. Chwastowski, A. Szczurek, Acta Phys. Polon. B **42**, 1861 (2011)
- [13] P. Lebiedowicz and A. Szczurek, Phys. Rev. D **81**, 036003 (2010)
- [14] P. Lebiedowicz, R. Pasechnik, A. Szczurek, Phys. Lett. B **701**, 434 (2011)
- [15] P. Lebiedowicz and A. Szczurek, Phys. Rev. D **85**, 014026 (2012)
- [16] P. Lebiedowicz and A. Szczurek, Phys. Rev. D **92**, 054001 (2015)
- [17] C. Ewerz, M. Maniatis, O. Nachtmann, Annals Phys. **342**, 31 (2014)
- [18] O. Nachtmann, Annals Phys. **209**, 436 (1991)
- [19] C. Ewerz, P. Lebiedowicz, O. Nachtmann, A. Szczurek, arXiv:1606.08067 [hep-ph].
- [20] L. Adamczyk *et al.* (STAR Collaboration), Phys. Lett. B **719**, 62 (2013)
- [21] P. Lebiedowicz, O. Nachtmann, A. Szczurek, Annals Phys. **344**, 301 (2014)
- [22] A. Bolz, C. Ewerz, M. Maniatis, O. Nachtmann, M. Sauter, A. Schöning, JHEP **1501**, 151 (2015)
- [23] P. Lebiedowicz, O. Nachtmann, A. Szczurek, Phys. Rev. D **91**, 074023 (2015)
- [24] F. Giacosa, this Proceedings
- [25] P. Lebiedowicz, O. Nachtmann, A. Szczurek, Phys. Rev. D **94**, 034017 (2016)
- [26] R. A. Kycia and J. Turnau, this Proceedings